Nanoscale

COMMUNICATION

View Article Online
View Journal | View Issue

Cite this: *Nanoscale*, 2016, **8**, 6948

Received 23rd December 2015,
Accepted 3rd March 2016

DOI: 10.1039/c5nr09158f

www.rsc.org/nanoscale

Time-evolution of *in vivo* protein corona onto blood-circulating PEGylated liposomal doxorubicin (DOXIL) nanoparticles†

Marilena Hadjidemetriou, Zahraa Al-Ahmady and Kostas Kostarelos*

Nanoparticles (NPs) are instantly modified once injected in the bloodstream because of their interaction with the blood components. The spontaneous coating of NPs by proteins, once in contact with biological fluids, has been termed the 'protein corona' and it is considered to be a determinant factor for the pharmacological, toxicological and therapeutic profile of NPs. Protein exposure time is thought to greatly influence the composition of protein corona, however the dynamics of protein interactions under realistic, *in vivo* conditions remain unexplored. The aim of this study was to quantitatively and qualitatively investigate the time evolution of *in vivo* protein corona, formed onto blood circulating, clinically used, PEGylated liposomal doxorubicin. Protein adsorption profiles were determined 10 min, 1 h and 3 h post-injection of liposomes into CD-1 mice. The results demonstrated that a complex protein corona was formed as early as 10 min post-injection. Even though the total amount of protein adsorbed did not significantly change over time, the fluctuation of protein abundances observed indicated highly dynamic protein binding kinetics.

Introduction

Nanoparticles (NPs) are thought to be instantly modified once injected in the bloodstream because of their tendency to interact with the surrounding blood constituents, of which proteins have been mostly studied today. The adsorption of proteins and their layering onto the surface of NPs has been termed the 'protein corona'.[1] This bio-transformation of nanomaterials has been postulated as a determinant factor for their overall biological behaviour and eventually their therapeutic efficacy.

The encapsulation of chemotherapeutic agents into phospholipid-based nanoscale vesicles, called liposomes, has been the most clinically established strategy to reduce the toxicity to normal tissues and simultaneously increase their accumulation into highly vascularised solid tumors.[2,3] Liposomal nanocarriers are being clinically used for more than 20 years, yet the effect of 'protein corona' formation on liposomal pharmacology is scarcely studied and far from being well understood. Despite the clinical use of liposomal doxorubicin (Doxil®)[4] and the increased interest in the study of serum protein corona formation around nanoparticles, there is currently no report in the literature describing the identification of proteins adsorbed onto blood circulating doxorubicin-encapsulated PEGylated liposomes. Such knowledge is needed not only to understand and predict liposomal pharmacology, but also to improve the existing, clinically-used formulations, often displaying relatively compromised therapeutic efficacy. The high-throughput proteomics analysis methods available today are powerful tools to comprehensively study protein corona profiles of clinically used nanoparticles.

In addition to the physiochemical characteristics of NPs, protein exposure time is thought to be a critical factor that shapes the composition of protein corona. The dynamics of protein interactions with macroscale surfaces was first described by Vroman in 1962,[5] suggesting a time-dependent association and dissociation of proteins. According to this model, highly abundant proteins, dominating at the early stage are later replaced by less abundant proteins with higher affinity for the surface. This description, referred to as the 'Vroman effect', shaped the hypothesis that protein corona formed onto the large surface area of NPs is a dynamic entity that evolves with time. There have been several *in vitro* investigations into the time evolution of protein corona.[6–8] Time-resolved characterisation of *in vitro* protein corona was recently comprehensively investigated for silica and polystyrene nanoparticles after the incubation with human plasma. In addition to 'Vroman' defined binding kinetics, authors described the existence of more complex, 'peak' or 'cup' shaped binding kinetics.[7] Despite the high-resolution quantitative LC-MS based proteomics employed and the insight offered,[7] the limitation of these studies lies on the *in vitro* design of the

Nanomedicine Lab, School of Medicine, Faculty of Medical & Human Sciences and National Graphene Institute, The University of Manchester, Manchester M13 9PT, UK. E-mail: kostas.kostarelos@manchester.ac.uk

†Electronic supplementary information (ESI) available. See DOI: 10.1039/C5NR09158F

interaction that fails to recognize the highly dynamic nature of blood and its heterogeneous flow velocity.

In a recent report,[9] we described a protocol to investigate the *in vivo* protein corona forming onto three different types of blood circulating liposome types (bare, PEGylated and targeted). The formation of *in vivo* protein corona was determined after the recovery of the liposomes from the blood circulation of CD-1 mice 10 min post-injection, whereas *in vitro* protein corona was determined after the incubation of liposomes in CD-1 mouse plasma. The differences between the protein coronas that formed *in vitro* and *in vivo* were revealed for the first time. The molecular complexity and morphology of the *in vivo* protein corona was shown not to be adequately predicted by the *in vitro* plasma incubation of NPs. Even though the total amount of protein attached on circulating liposomes correlated with that observed from *in vitro* incubations, the variety of molecular species in the *in vivo* corona was considerably wider. However, one of the limitations of that study was that the liposome systems studied (even though all constituted vesicles that have been clinically trialed) did not encapsulate any therapeutic agent. In addition, due to the short half-life of bare (non-PEGylated) liposomes employed, we chose to investigate corona formation at a single time point (10 min post-incubation).

In this study, we attempted to investigate the time evolution of protein corona under realistic *in vivo* conditions. Given the lack of protein corona investigations for clinically used liposomes, we employed PEGylated liposomal doxorubicin, identical to the clinical product intravenously infused in patients. The drug-loaded vesicles were injected into CD1 mice and recovered from the blood circulation 10 min, 1 h and 3 h post-injection. The protein coronas formed at these three different time points were qualitatively and quantitatively characterized and compared (Fig. 1).

Results and discussion

The chemical composition and the physicochemical characteristics of doxorubicin-encapsulated PEGylated liposomes that were fabricated for this study are summarized in Table S1.† The lipid composition and molar ratios of the individual lipid bilayer components were chosen to match the exact liposome composition of the clinically-used liposomal doxorubicin agent Doxil®. Dynamic light scattering (DLS), ζ-potential measurements and negative stain transmission electron microscopy (TEM) were performed prior to intravenous administration of liposomes to access their properties and morphology. Liposomes had a mean hydrodynamic diameter of 115 nm, a negative surface charge of −36 mV and displayed low polydispersity values (<0.06) indicating a narrow size distribution (Fig. 2A). TEM imaging showed well-dispersed, round shaped vesicles, with their size correlating that of DLS measurements (Fig. 2B and C).

To obtain a time-dependent investigation of the *in vivo* formed protein corona, liposomes were intravenously administered *via* tail vein injection into CD-1 mice and recovered by cardiac puncture 10 min, 1 h and 3 h post-injection, as shown in Fig. 1. Plasma was then prepared from recovered blood by centrifugation (see Experimental section for further details). A protocol combining size exclusion chromatography and membrane ultrafiltration was used for the isolation of liposome-corona complexes from unbound and loosely bound plasma proteins, as previously described.[9] This protocol allows only the retention of the tightly adsorbed proteins onto the liposome surface, also referred by some as the 'hard corona'.[10]

Dynamic light scattering measurements of protein corona-coated liposomes demonstrated that their size distribution broadened (larger polydispersity index), while their surface charge remained negative (Fig. 2A and Table S1†). In agreement with previous studies investigating liposomal protein corona formation, we observed a blood-induced reduction in the mean diameter of liposomes, consistent with all different time points of investigation (Fig. 2A and Table S1†).[9,11] This osmotically-driven shrinkage was attributed to the high elastic deformation of liposomes, however it was also observed here for doxorubicin-loaded vesicles without content loss as evidenced by cryo-EM (Fig. 2C). In addition, TEM revealed well-dispersed liposomes that retained their structural integrity after recovery, while the presence of the protein molecules adsorbed onto their surface revealed protein corona formation, as early as 10 min-post injection (Fig. 2B and S1†). In agreement with our previous cryo-EM studies, the *in vivo* protein corona did not appear to coat all the available liposome surfaces entirely[9] (Fig. 2C).

Based on established pharmacokinetic data for the clinically-used PEGylated liposomes encapsulating doxorubicin,[12–15] we knew that 40% of injected dose will remain in circulation for at least 6 hours. As a first step towards elucidation of the time evolution of the protein corona we quantitatively compared the coronas formed around the drug-encapsulated PEGylated vesicles at three different exposure times. To compare the total amount of protein adsorbed, we calculated the protein binding ability (Pb), defined as the amount of protein associated with each μmole of lipid. As shown in Fig. 3A, Pb values determined at the earliest exposure time (t = 10 min) did not significantly change even after the longest blood exposure time (t = 3 h). This data indicated that liposome-specific protein fingerprints were already established by the earliest time point (t = 10 min) and any possible qualitative changes in the composition of protein corona over time would be a result of a competitive exchange process. Pb values observed for doxorubicin encapsulated liposomes, were slightly higher than Pb values determined in our previous study for empty liposomes of the same composition.[9] This could be attributed to the different mass and blood flow dynamics of these vesicles after the encapsulation of doxorubicin. Whether a second layer of proteins with low adherence, sometimes termed as 'soft corona', exists or not remains to be proven and could not be resolved by our analytical approach.

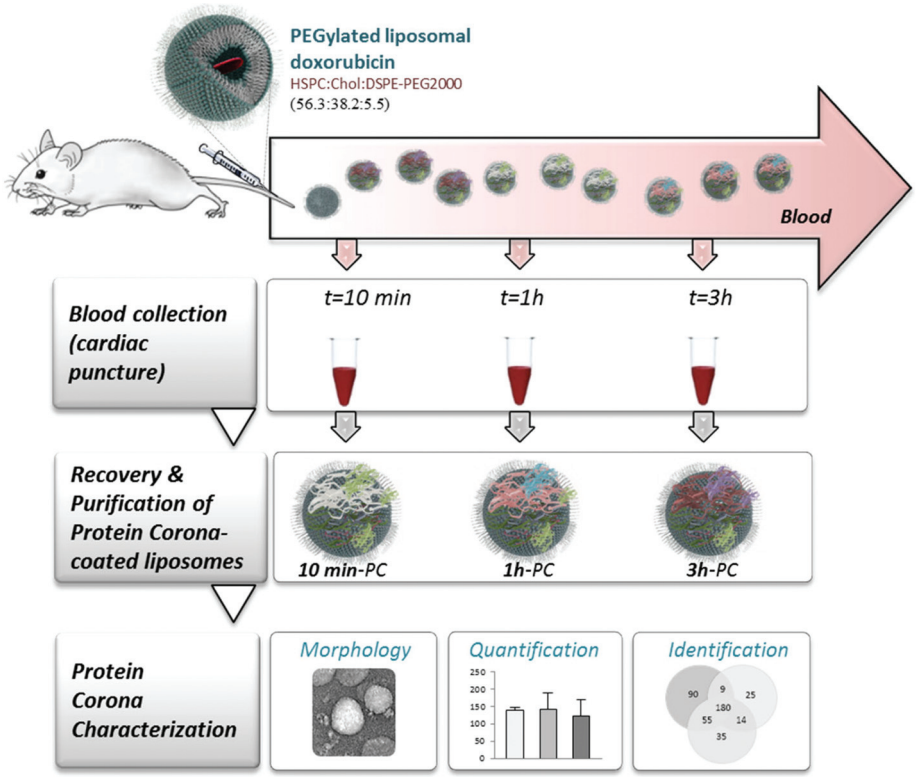

Fig. 1 Schematic Description of the experimental design. To obtain a time-dependent investigation of the *in vivo* formed protein corona (PC), liposomes were intravenously administered *via* tail vein injection into CD-1 mice (n = 3 mice per group; 3 independent experiments replicated) and recovered by cardiac puncture 10 min, 1 h and 3 h post-injection. The plasma was then separated from the recovered blood by centrifugation. *In vivo* protein-coated liposomes were purified from unbound proteins and protein coronas formed at these three different time points were qualitatively and quantitatively characterized and compared.

A comprehensive identification of proteins associated with liposomes was then performed by mass spectrometry. The Venn diagram in Fig. 3B illustrates the number of common and unique proteins between the coronas formed after the three different time points of recovery. As already evident from the quantification of total protein adsorbed (Fig. 3A), a complex protein corona was determined at the earliest time point (t = 10 min), with 334 identified proteins (Fig. 3B). The majority of identified proteins (n = 180) were common between the three time points. 90 unique proteins were identified for the 10 min-formed corona, whereas 25 and 35 unique proteins were present in the coronas of 1 h and 3 h recovered liposomes, respectively. It should be noted that the majority of unique proteins belonged to the group of low abundance, as revealed by the Relative Protein Abundance (RPA) values determined for each of the identified proteins. Previous *in vitro* investigations suggested that protein corona reaches its final equilibrium 1 h post-incubation of NPs with plasma proteins.[6] Barran-Berdon *et al.* employed mass spectrometry to show that protein corona, formed onto cationic liposomes incubated with human plasma, forms rapidly (t = 1 min) and stops evolving 1 h post-incubation.[6] Our study demonstrated that the *in vivo* protein corona continues to evolve over time, even at 3 h post-injection (Fig. 3B). These contradictory results are not surprising, considering the complexity of the physiological environment, the potential effect of blood flow dynamics on the *in vivo* formation of the protein corona, as well as the role of possible NP-triggered immune responses that may cause variations in the blood composition over time.

Pozzi D *et al.*,[16] have previously showed that the *in vitro* incubation of empty liposomes with fetal bovine serum (FBS) under static and flow conditions led to protein coronas of different composition. Interestingly, dynamic (flow) conditions promoted the extensive adherence of low molecular weight (MW) proteins, in comparison to incubation under static conditions. To investigate whether the previous observation applies also under the more realistic, dynamic *in vivo* conditions of blood flow, bound proteins were classified according to their molecular mass (Fig. 3C). In agreement with the study by Pozzi *et al.*,[16] there was a tendency towards interaction with low MW proteins. Plasma proteins with MW < 80 accounted for more than 80% of the protein coronas formed 10 min, 1 h and 3 h post-injection. Notably, a fluctuation in the contribution of each protein group (classified based on MW) on the corona composition was observed over time. For instance, ~40% of associated proteins had a MW < 20 at 10 min and 3 h time points, whereas the contribution of this group was significantly lower 1 h post-injection (~25%),

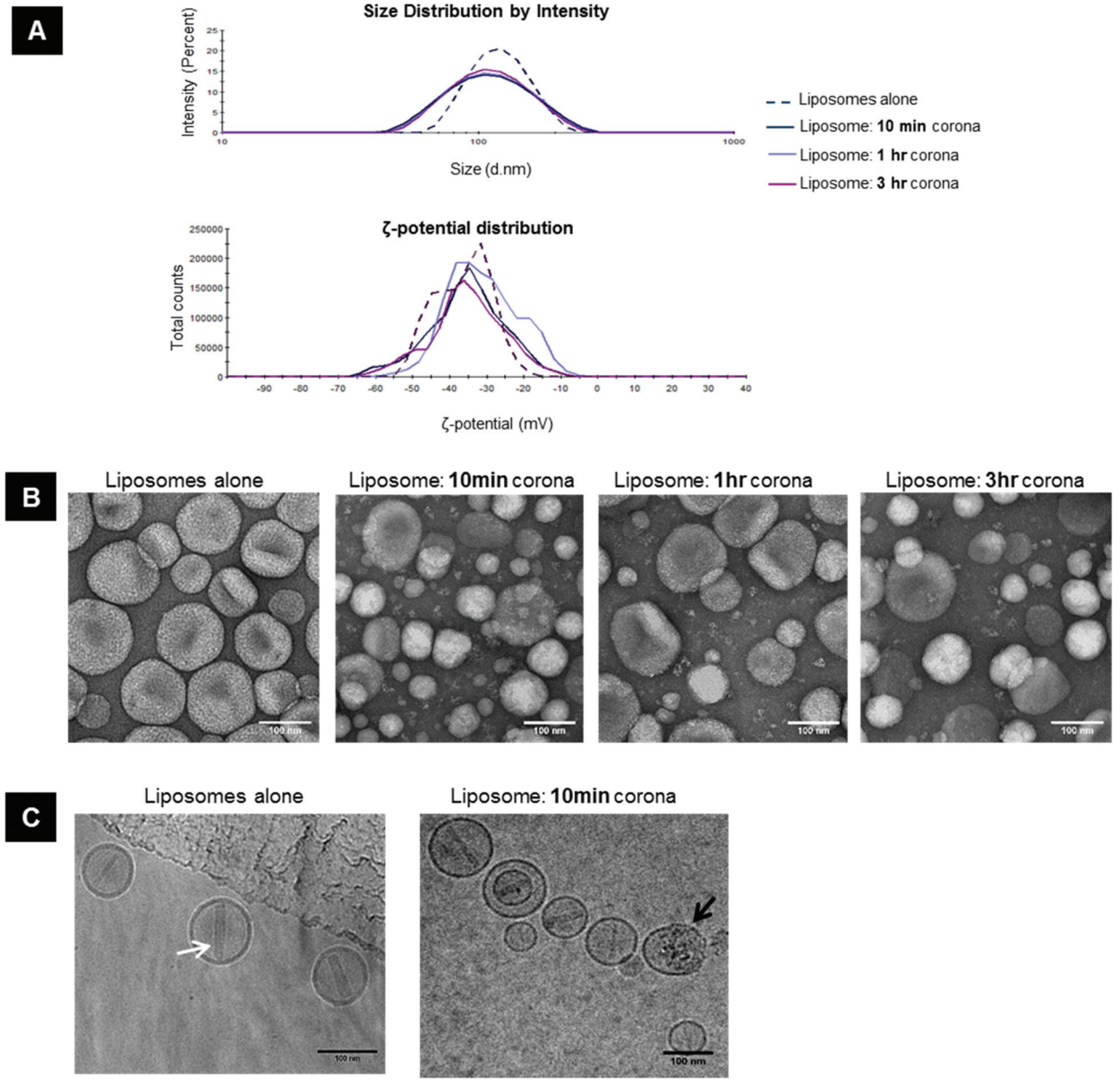

Fig. 2 The effect of protein corona formation on the physicochemical characteristics and morphology of liposomes. (A) Mean diameter (nm) and ζ-potential (mV) distributions and (B) Negative stain TEM imaging of liposomes before their interaction with plasma proteins and 10 min, 1 h and 3 h after their i.v. injection and recovery from CD-1 mice. (C) Cryo-EM imaging of doxorubicin-encapsulating (white arrow) liposomes before injection and recovered after 10 min in blood circulation, partially coated with plasma proteins (black arrow). All scale bars are 100 nm.

indicating the dynamic character of the *in vivo* protein corona (Fig. 3C).

To better understand the time evolution of the *in vivo* protein corona, the relative protein abundance (RPA) of each identified protein was determined. Fig. 4A summarizes the 20 most abundant proteins associated with the surface of liposomes 10 min, 1 h and 3 h after their intravenous administration. Blood exposure time was found to be a significant factor influencing liposome-bound protein abundance. Common proteins observed in the Venn diagram of Fig. 3B were not equally abundant (Fig. 4). A striking observation was that the most abundant protein of the three coronas formed at different time points were not identical. Alpha-2 macroglobulin had the highest RPA value 10 min post-injection, while apolipoprotein E and hemoglobin beta-1 were the most abundant proteins in the coronas of 1 h and 3 h blood-circulating liposomes, respectively. Lipoproteins were found to be the most abundant class of proteins, contributing to ~20% of the 10 min-formed protein corona (Fig. 4B), followed by immunoglobulins (RPA ~ 15%) and complement proteins (RPA ~ 5%) (Fig. 4C and D).

Doxorubicin-encapsulated, PEGylated liposomes, employed in this study, were designed to have a prolonged blood circulation half-life which enhances their possibility to extravasate

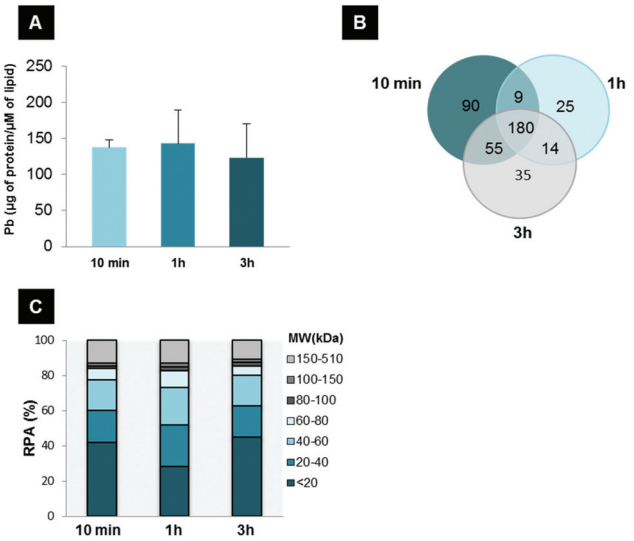

Fig. 3 Characterization of *in vivo* protein corona: (A) comparison of the total amount of proteins adsorbed *in vivo* onto liposomes recovered from CD1 mouse circulation 10 min, 1 h and 3 h post-injection. Pb values (µg of protein per µM lipid) represent the average and standard error from three independent experiments, each using three mice; (B) Venn diagrams report the number of unique proteins identified in the *in vivo* corona formed 10 min, 1 h and 3 h post-injection and their respective overlap; (C) classification of the corona proteins identified according to their molecular mass.

through the leaky tumor vasculature.[2] There have been several proposed mechanisms to explain the prolonged circulation of PEGylated nanovehicles. In agreement with previous reports, this study demonstrated that PEGylated surfaces are not completely inert and interact with the blood components *in vivo*.[17–19] Even though PEGylation reduces the total amount of proteins adsorbed,[9] the presence of opsonins (complement proteins and immunoglobulins) in their protein coronas (Fig. 4) may be thought to contradict with their long-circulating profile. The concept of 'dys-opsonization' has been proposed to describe the adsorption of proteins that extend the circulation time of liposomes.[20] Lipoproteins identified in this study as the most abundant proteins (Fig. 4B), have been suggested to have dys-opsonic activity, possibly explained by their competitive binding with opsonic proteins. Also, the PEG-mediated inhibition of liposome interaction with circulating cells has been suggested, based on previous *in vitro* studies reporting reduced internalization of liposomes after PEGylation.[21] According to this scenario, the identity of the protein corona seems to have a minor impact on the overall biodistribution profile of PEGylated liposomes.

As illustrated in Fig. 4D, the *in vivo* protein coronas formed at the three different time points, consisted of several key complement cascade proteins, involved in the classical (complement C1q, C4b), alternative (complement factor h) and lectin (mannan-binding lectin serine protease, mannose-binding lectin) pathways of activation.[22] The impact of complement activation on the potential adverse effects of liposomes had been valued before the term 'protein corona' was introduced.[23] Immediately after intravenous infusion, PEGylated liposomal doxorubicin has been previously shown to interact with the complement system causing transient and in most of the cases mild hypersensitive reactions, termed as C-activation related pseudoallergy (CARPA).[24,25] Chanan-Khan *et al.* reported that 45% of cancer patients (n = 29) treated for the first time with Doxil® experienced hypersensitivity reactions associated by complement activation.[24] Plasma levels of protein-s bound C terminal complex (SC5B-9) have been traditionally used as an indicator of complement activation.[24] However, correlations between material properties and complement activation were difficult to be made without thorough identification of adhered proteins. *In vivo* protein corona fingerprinting offers a new tool for molecular investigation of nanoparticle-triggered complement events and the consequences arising from them and more work would be needed to explore this further. However, it is also important to appreciate the potential limitations of extrapolating immune system data from mice to humans.[26]

To gain some further understanding of the protein binding kinetics occurring *in vivo* after the intravenous administration of NPs, we classified the most abundant liposome-bound proteins into 5 groups according to the fluctuation of their normalized protein abundance value over time (Fig. S2†). In agreement with the 'Vroman effect' theory, some proteins replaced or were replaced by others exhibiting increased (Fig. S2A†) or reduced (Fig. S2B†) binding over time, respectively. For instance, the abundance of fibrinogen in the protein corona formed 3 h post-injection was 5 times greater in comparison with the abundance observed for the 10 min-formed corona. Tenzer and co-workers were the first to describe the existence of more complex, 'peak' or 'cup' shaped binding kinetics after the *in vitro* incubation of silica and polystyrene NPs with human plasma.[7] Similarly, we observed proteins characterized by low abundance at the beginning of blood circulation (t = 10 min) and at later time points (t = 3 h), but displaying peak abundance at intermediate time points (t = 1 h) (Fig. S2C†) or *vice versa* (Fig. S2D†). In addition to the above mentioned binding kinetic groups we also observed proteins that retained their abundance over time (Fig. S2E†). The sum of all the binding kinetic processes observed, resulted in a constant total amount of protein on the surface of liposomes over time (Fig. 2A). Such observations are of great importance to comprehensively understand the overall performance of already clinically established formulations. We have previously shown that almost 40% and 15% of the injected liposomal doxorubicin remains in the blood after 6 h and 24 h, respectively.[13] This suggests that liposomes extravasate at the tumor tissue at different time points post-injection. It has been also shown that the drug release profiles,[27] as well as the interaction of liposomes with cells,[28,29] are greatly affected by the proteins adsorbed onto their surfaces. Therefore, the *in vivo*, highly dynamic protein binding kinetics, demonstrated in this study, could result in altered therapeutic efficacy of liposomes over time.

A

10 min		1 hr		3 hr	
Identified Protein	**RPA**	**Identified Protein**	**RPA**	**Identified Protein**	**RPA**
Alpha-2-macroglobulin	8.02 ± 1.45	Apolipoprotein E (PE=2 SV=1)	8.19 ± 1.71	Hemoglobin subunit beta-1	8.58 ± 1.93
Apolipoprotein C-III	6.37 ± 0.73	Alpha-2-macroglobulin	7.66 ± 1.06	Apolipoprotein E (PE=2 SV=1)	7.30 ± 0.27
Hemoglobin subunit beta-1	5.79 ± 0.13	Apolipoprotein C-III	4.86 ± 1.68	Apolipoprotein C-III	6.65 ± 0.69
Apolipoprotein E (PE=1 SV=2)	5.57 ± 0.33	Serum albumin	4.41 ± 1.74	Alpha-2-macroglobulin	6.42 ± 0.99
Beta-globin, Hbbt1 (A8DUK2)	4.48 ± 0.16	Apolipoprotein E (PE=1 SV=2)	3.87 ± 3.87	Beta-globin, Hbbt1 (A8DUK2)	6.02 ± 1.36
Apolipoprotein A-I	3.31 ± 0.27	Hemoglobin subunit beta-1	3.82 ± 0.16	Hemoglobin subunit beta-2	4.54 ± 1.09
Hemoglobin subunit beta-2	2.93 ± 0.13	Apolipoprotein A-I	3.25 ± 1.00	Alpha-globin	3.77 ± 0.89
Alpha-globin	2.74 ± 0.01	Serine protease inhibitor A3K	2.63 ± 0.93	Apolipoprotein A-I	2.14 ± 0.96
Ig mu chain C region	2.62 ± 0.21	Ig mu chain C region	2.23 ± 0.29	Fibrinogen beta chain	1.98 ± 0.61
Putative uncharacterized protein	2.54 ± 0.06	Hemoglobin subunit beta-2	2.20 ± 0.24	Fibrinogen gamma chain	1.92 ± 0.53
Serum albumin	2.35 ± 0.40	Alpha-globin	1.97 ± 0.53	Putative uncharacterized protein	1.68 ± 1.68
APOAII	1.89 ± 0.01	Serotransferrin	1.73 ± 0.64	Ig mu chain C region	1.56 ± 0.25
If kappa light chain (Fragment)	1.16 ± 0.11	Beta-globin, Hbbt1 (A8DUK2)	1.30 ± 1.30	Serum albumin	1.50 ± 0.59
Serine protease inhibitor A3K	1.14 ± 0.07	Complement C3	1.24 ± 0.43	Fibrinogen alpha chain	1.40 ± 0.53
Complement C3	0.95 ± 0.10	Aberrantly recombined kappa chain	1.10 ± 0.08	Serine protease inhibitor A3K	1.27 ± 0.50
Protein Ighv7-1	0.94 ± 0.11	Alpha-1B-glycoprotein	1.09 ± 0.34	If kappa light chain (Fragment)	1.18 ± 0.07
Serotransferrin	0.93 ± 0.08	APOAII	1.04 ± 0.31	APOAII	1.01 ± 0.05
Mannose-binding protein C	0.91 ± 0.03	If kappa light chain (Fragment)	1.02 ± 0.14	Protein Ighv7-1	0.96 ± 0.19
Apolipoprotein B-100	0.91 ± 0.06	Apolipoprotein B-100	0.97 ± 0.06	Protein Ighv1-18	0.94 ± 0.12
Ig lambda-2 chain C region	0.90 ± 0.76	Protein Ighv7-1	0.95 ± 0.18	Apolipoprotein B-100	0.92 ± 0.10
Anti-colorectal carcinoma light chain	0.86 ± 0.43	Alpha-1-antitrypsin 1-3	0.94 ± 0.26	Anti-colorectal carcinoma light chain	0.85 ± 0.43

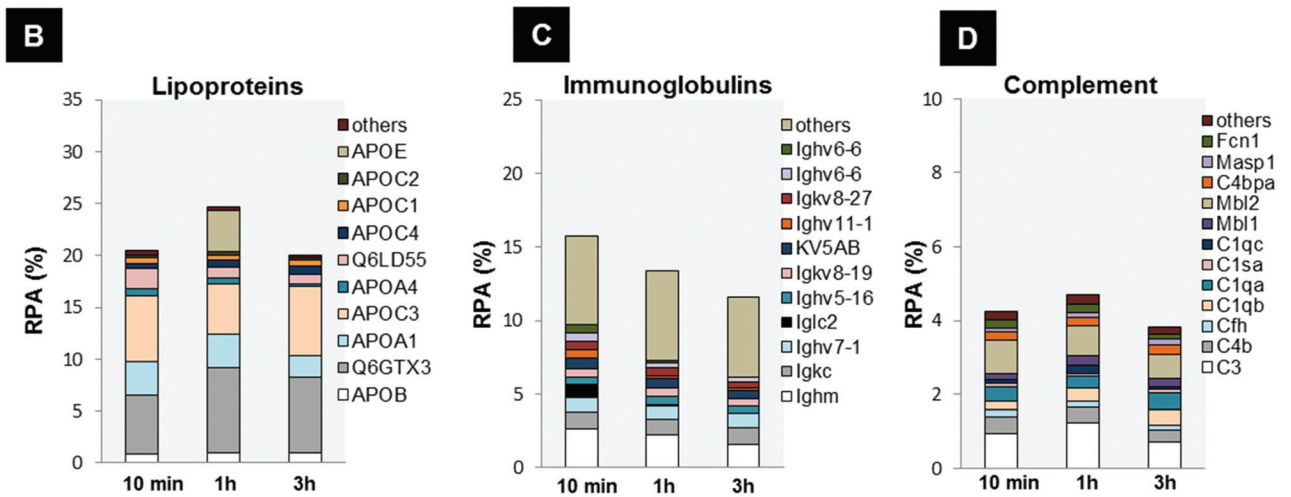

Fig. 4 Time evolution of *in vivo* protein corona: (A) most-abundant proteins (top-20) identified in the protein corona of PEGylated liposomal doxorubicin 10 min, 1 h and 3 h post-injection by LC-MS/MS. Relative protein abundance (RPA) values represent the average and standard error from three independent experiments; (B) the relative percentage of lipoproteins, immunoglobulins and complement proteins identified in the protein corona 10 min, 1 h and 3 h post-injection.

On a broader context, we propose that understanding the biological impact of *in vivo* forming protein corona is crucial for the rational design of new formulations, with improved therapeutic efficacy. Much work has been done concerning the effect of protein corona on the interaction of NPs with cells, suggesting that protein adsorption can either facilitate[30] or inhibit[31] cellular uptake. The observation that the targeting capabilities of nanoscale constructs are diminished while in

blood circulation because of their interaction with plasma proteins[31] has also led to the idea of exploiting the protein corona in order to direct them to specific target cells. According to this strategy, NPs can be specifically designed to interact with proteins that will initiate targeted receptor mediated endocytosis.[30] However, a comprehensive characterization of protein corona under physiological conditions is necessary before exploring its potential exploitation for targeting purposes. Blood flow dynamics, although a great influential factor for nanoparticle–protein interactions, seem to be largely ignored in the protein corona literature. In our previous study, we demonstrated that the complexity of *in vivo* formed protein corona cannot be adequately predicted by *in vitro* plasma incubations.[9] In addition, data in this study suggest that *in vivo* characterization of the protein corona at a single time point is insufficient to describe the surface modifications that nanoparticles experience *in vivo*. The fluctuation in the abundance of each identified protein, observed over time, reveals that the formation of protein corona in a controlled and predictable manner, as often suggested, is challenging, if not physiologically unrealistic.

Conclusion

This is the first study to investigate the time evolution of protein corona under realistic *in vivo* conditions. Protein adsorption profiles were determined at three different time points post-injection (10 min, 1 h and 3 h) of PEGylated liposomal doxorubicin, clinically used for the treatment of various neoplastic conditions. The results demonstrated that a complex protein corona was formed as early as 10 min post-injection. Even though the total amount of protein adsorbed did not significantly change, the abundance of each protein identified fluctuated over time indicating that competitive exchange processes were taking place. We anticipate that comprehensive identification of protein coronas under realistic *in vivo* conditions for different types of blood-injected pharmacological agents that lie in the nanoscale is necessary to improve our understanding of their overall clinical performance.

Experimental

Materials

Hydrogenated soy phosphatidylcholine (HSPC), 1,2-distearoyl-*sn*-glycero-3-phosphoethanolamine-*N*-[methoxy(polyethylene glycol)-2000] (DSPE-PEG2000) and 1,2-distearoyl-*sn*-glycero-3-phosphoethanolamine-*N*-[maleimide(polyethylene glycol)-2000] (ammonium salt) (Mal-DSPE-PEG2000) were purchased from Avanti Polar Lipids (USA), while doxorubicin hydrochloride, cholesterol and 4-(2-hydroxyethyl) piperazine-1-ethanesulfonic acid (HEPES) were purchased from Sigma (UK).

Preparation of PEGylated liposomal doxorubicin nanoparticles

Liposomes were prepared by thin lipid film hydration method followed by extrusion. Table S1† shows the liposomal formulation employed, the lipid composition and the molar ratios. Briefly, lipids of different types were dissolved in chloroform : methanol mixture (4 : 1) in a total volume of 2 ml, using a 25 ml round bottom flask. Organic solvents were then evaporated using a rotary evaporator (Buchi, Switzerland) at 40 °C, at 150 rotations per min, 1 h under vacuum. Lipid films were hydrated with ammonium sulphate 250 mM (pH 8.5) at 60 °C to produce large multilammer liposomes. Small unilamellar liposomes were then produced by extrusion though 800 nm and 200 nm polycarbonate filters (Whatman, VWR, UK) 10 times each and then 15 times through 100 nm and 80 nm extrusion filters (Whatman, VWR, UK) using a mini-Extruder (Avanti Polar Lipids, Alabaster, AL).

For DOX loading, the ammonium sulphate gradient method was used. Exchanging the external unencapsulated ammonium sulphate was performed by gel filtration through Sepharose CL-4B column (15 cm × 1.5 cm) (Sigma, UK) equilibrated with HBS (pH 7.4). Doxorubicin hydrochloride was added to the liposome suspensions at 1 : 20 DOX : lipids mass ratio in respect to the original total lipid concentration. Subsequently, samples were incubated at 60 °C for 1 h. After incubation, liposomes were passed through PD-10 desalting columns (GE Healthcare Life Sciences) to remove any free DOX.

Animal experiments

Eight to ten week old female CD1 mice were purchased from Charles River (UK). Animal procedures were performed in compliance with the UK Home Office Code of Practice for the Housing and Care of Animals used in Scientific Procedures. Mice were housed in groups of five with free access to water and kept at temperature of 19–22 °C and relative humidity of 45–65%. Before performing the procedures, animals where acclimatized to the environment for at least 7 days.

Protein corona formation after *in vivo* administration

CD1 mice were anesthetized by inhalation of isoflurane and liposomes were administered intravenously *via* the lateral tail vein, at a lipid dose of 0.125 mM g^{-1} body weight to achieve a final doxorubicin dose of 5 mg kg^{-1} body weight, used for preclinical studies.[32–34] 10 minutes, 1 h and 3 h post-injection, blood was recovered by cardiac puncture using K2EDTA coated blood collection tubes. Approximately 0.5–1 ml of blood was recovered from each mouse. Plasma was prepared by inverting 10 times the collection tubes to ensure mixing of blood with EDTA and subsequent centrifugation for 12 minutes at 1300 RCF at 4 °C. Supernatant was collected into Protein LoBind Eppendorf Tubes. For each time point the plasma samples obtained from three mice were pooled together for a final plasma volume of 1 ml. Three experimental replicates were performed and therefore 9 mice were used in total for each time point.

Separation of corona-coated liposomes from unbound and weakly bound proteins

Liposomes recovered from *in vivo* experiments were separated form excess plasma proteins by size exclusion chromatography followed by membrane ultrafiltration, as we have previously described.[9] Immediately after the *in vivo* incubations, 1 ml of plasma samples was loaded onto a Sepharose CL-4B (SIGMA-ALDRICH) column (15 × 1.5 cm) equilibrated with HBS. Chromatographic fractions 4,5 and 6 containing liposomes were then pooled together and concentrated to 500 μl by centrifugation using Vivaspin 6 column (10 000 MWCO, Sartorious, Fisher Scientific) at 3000 rpm. Vivaspin 500 centrifugal concentrator (1 000 000 MWCO, Sartorious, Fisher Scientific) was then used at 3000 rpm, to further concentrate the samples to 100 μl and to ensure separation of protein-coated liposomes from the remaining large unbound proteins. Liposomes were then washed 3 times with 100 μl HBS to remove weekly bound proteins.

Size and zeta potential measurements using dynamic light scattering (DLS)

Liposome size and surface charge were measured using Zetasizer Nano ZS (Malvern, Instruments, UK). For size measurement, samples were diluted with distilled water in 1 ml cuvettes. Zeta potential was measured in disposable Zetasizer cuvettes and sample dilution was performed with distilled water. Size and zeta potential data were taken in three and five measurements, respectively.

Transmission electron microscopy (TEM)

Liposomes of different composition were visualized with transmission electron microscopy (FEI Tecnai 12 BioTwin) before and after their *in vivo* interaction with plasma proteins. Samples were diluted to 1 mM lipid concentration, then a drop from each liposome suspension was placed onto a Carbon Film Mesh Copper Grid (CF400-Cu, Electron Microscopy Science) and the excess suspension was removed with a filter paper. Staining was performed using aqueous uranyl acetate solution 1%.

Cryo-electron microscopy

TEM grids of liposomes were prepared in a FEI Vitrobot using 3 μl of sample absorbed to freshly glow-discharged R2/2 Quantifoil grids. Grids were continuously blotted for 4–5 s in a 95% humidity chamber before plunge-freezing into liquid ethane. Data were then recorded on a Polara F30 FEG operating at 200 kV on a 4 K Gatan Ultrascan CCD (charge-coupled device) in low-dose mode. CD images were recorded between 0.5 and 5.0 μm defocus at a normal magnification of 39 000× and at 3.5 Å per pixel (1 Å = 0.1 nm) and had a maximum electron dose of <25 electrons per $Å^2$.

Quantification of adsorbed proteins

Proteins associated with recovered liposomes were quantified by BCA Protein assay kit. Pb values, expressed as μg of protein per μM lipid were then calculated and represented as the average ± standard error of three independent experiments. For the BCA assay, a 6-point standard curve was generated by serial dilutions of BSA in HBS, with the top standard at a concentration of 2 μg ml^{-1}. BCA reagent A and B were mixed at a ratio of 50 : 1 and 200 μl of the BCA mixture were dispensed into a 96-well plate, in duplicates. Then, 25 μl of each standard or unknown sample were added per well. The plate was incubated for 30 minutes at 37 °C, after which the absorbance was read at 574 nm on a plate reader (Fluostar Omega). Protein concentrations were calculated according to the standard curve. To quantify lipid concentration, 20 μl of each samples was mixed with 1 ml of chloroform and 500 μl of Stewart assay reagent in an Eppendorf tube. The samples were vortexed for 20 seconds followed by 1 min of centrifugation at 13 000 RPM. 200 μl of the chloroform phase was transferred to a quartz cuvette. The optical density was measured on a using Cary 50 Bio Spectrophotometer (Agilent Technologies) at 485 nm. Lipid concentration was calculated according to a standard curve.

Mass spectrometry

Proteins associated with 0.05 μM of liposomes were mixed with Protein Solving Buffer (Fisher Scientific) for a final volume of 25 μl and boiled for 5 minutes at 90 °C. Samples were then loaded in 10% Precise Tris-HEPES Protein Gel (Thermo Scientific). The gel was run for 3–5 minutes 100 V, in 50 times diluted Tris-HEPES SDS Buffer (Thermo Scientific). Staining was performed with EZ Blue™ Gel Staining reagent (Sigma Life Science) overnight followed by washing in distilled water for 2 h. Bands of interest were excised from the gel and dehydrated using acetonitrile followed by vacuum centrifugation. Dried gel pieces were reduced with 10 mM dithiothreitol and alkylated with 55 mM iodoacetamide. Gel pieces were then washed alternately with 25 mM ammonium bicarbonate followed by acetonitrile. This was repeated, and the gel pieces dried by vacuum centrifugation. Samples were digested with trypsin overnight at 37 °C.

Digested samples were analysed by LC-MS/MS using an UltiMate® 3000 Rapid Separation LC (RSLC, Dionex Corporation, Sunnyvale, CA) coupled to Orbitrap Velos Pro (Thermo Fisher Scientific) mass spectrometer. Peptide mixtures were separated using a gradient from 92% A (0.1% FA in water) and 8% B (0.1% FA in acetonitrile) to 33% B, in 44 min at 300 nL min^{-1}, using a 250 mm × 75 μm i.d. 1.7 μM BEH C18, analytical column (Waters). Peptides were selected for fragmentation automatically by data dependant analysis. Data produced were searched using Mascot (Matrix Science UK), against the [*Uniprot*] database with taxonomy of [*mouse*] selected. Data were validated using Scaffold (Proteome Software, Portland, OR).

The Scaffold software (version 4.3.2, Proteome Software Inc.) was used to validate MS/MS based peptide and protein identifications and for relative quantification based on spectral counting. Peptide identifications were accepted if they could be established at greater than 95.0% probability by the Peptide

Prophet algorithm with Scaffold delta-mass correction. Protein identifications were accepted if they could be established at greater than 99.0% probability and contained at least 2 identified peptides. Protein probabilities were assigned by the Protein Prophet algorithm. Proteins that contained similar peptides and could not be differentiated based on MS/MS analysis alone were grouped to satisfy the principles of parsimony. Semi quantitative assessment of the protein amounts was conducted using normalized spectral countings, NSCs, provided by Scaffold Software. The mean value of NSCs obtained in the three experimental replicates for each protein was normalized to the protein MW and expressed as a relative quantity by applying the following equation:[17]

$$\mathrm{MWNSC_k} = \frac{(\mathrm{NSC/MW})_k}{\sum_{i=1}^{N} (\mathrm{NSC/MW})_i \times 100}$$

where, MWNSCk is the percentage molecular weight normalized NSC for protein k and MW is the molecular weight in kDa for protein k. This equation takes into consideration the protein size and evaluates the contribution of each protein reflecting its relative protein abundance (RPA).

Statistical analysis

Statistical analysis of the data was performed using IBM SPSS Statistics software. One-way analysis of variance (ANOVA) followed by the Tukey multiple comparison test were used and p values <0.05 were considered significant.

Conflict of interest

The authors declare no competing financial interest.

Author contributions

M. Hadjidemetriou designed and performed all experiments and took responsibility for planning and writing the manuscript. Z. Al-ahmady contributed in the intravenous administration of liposomes and blood collection. K. Kostarelos initiated, designed, directed, provided intellectual input and contributed to the writing of the manuscript.

Acknowledgements

This research was partially funded by the Marie Curie Initial Training Network *PathChooser* (PITN-GA-2013-608373). The authors also wish to thank the staff in the Faculty of Life Sciences EM Facility for their assistance and the Wellcome Trust for equipment grant support to the EM Facility. In addition, Mass Spectrometry Facility staff at the University of Manchester for their assistance and Mr M. Sylianides for his help with the TOC image and liposome illustration.

References

1 T. Cedervall, I. Lynch, S. Lindman, T. Berggard, E. Thulin, H. Nilsson, K. A. Dawson and S. Linse, Understanding the nanoparticle-protein corona using methods to quantify exchange rates and affinities of proteins for nanoparticles, *Proc. Natl. Acad. Sci. U. S. A.*, 2007, **104**, 2050–2055.

2 K. M. Laginha, S. Verwoert, G. J. Charrois and T. M. Allen, Determination of doxorubicin levels in whole tumor and tumor nuclei in murine breast cancer tumors, *Clin. Cancer Res.*, 2005, **11**, 6944–6949.

3 T. Safra, F. Muggia, S. Jeffers, D. D. Tsao-Wei, S. Groshen, O. Lyass, R. Henderson, G. Berry and A. Gabizon, Pegylated liposomal doxorubicin (doxil): reduced clinical cardiotoxicity in patients reaching or exceeding cumulative doses of 500 mg/m2, *Ann. Oncol.*, 2000, **11**, 1029–1033.

4 Y. Barenholz, Doxil(R)–the first FDA-approved nano-drug: lessons learned, *J. Controlled Release*, 2012, **160**, 117–134.

5 L. Vroman, Effect of Adsorbed Proteins on Wettability of Hydrophilic and Hydrophobic Solids, *Nature*, 1962, **196**, 476–477.

6 A. L. Barran-Berdon, D. Pozzi, G. Caracciolo, A. L. Capriotti, G. Caruso, C. Cavaliere, A. Riccioli, S. Palchetti and A. Lagana, Time evolution of nanoparticle-protein corona in human plasma: relevance for targeted drug delivery, *Langmuir*, 2013, **29**, 6485–6494.

7 S. Tenzer, D. Docter, J. Kuharev, A. Musyanovych, V. Fetz, R. Hecht, F. Schlenk, D. Fischer, K. Kiouptsi, C. Reinhardt, K. Landfester, H. Schild, M. Maskos, S. K. Knauer and R. H. Stauber, Rapid formation of plasma protein corona critically affects nanoparticle pathophysiology, *Nat. Nanotechnol.*, 2013, **8**, 772–781.

8 E. Casals, T. Pfaller, A. Duschl, G. J. Oostingh and V. Puntes, Time Evolution of the Nanoparticle Protein Corona, *ACS Nano*, 2010, **4**, 3623–3632.

9 M. Hadjidemetriou, Z. Al-Ahmady, M. Mazza, R. F. Collins, K. Dawson and K. Kostarelos, In Vivo Biomolecule Corona around Blood-Circulating, Clinically Used and Antibody-Targeted Lipid Bilayer Nanoscale Vesicles, *ACS Nano*, 2015, **9**, 8142–8156.

10 M. P. Monopoli, C. Aberg, A. Salvati and K. A. Dawson, Biomolecular coronas provide the biological identity of nanosized materials, *Nat. Nanotechnol.*, 2012, **7**, 779–786.

11 J. Wolfram, K. Suri, Y. Yang, J. Shen, C. Celia, M. Fresta, Y. Zhao, H. Shen and M. Ferrari, Shrinkage of pegylated and non-pegylated liposomes in serum, *Colloids Surf., B*, 2014, **114**, 294–300.

12 A. Gabizon, H. Shmeeda and Y. Barenholz, Pharmacokinetics of pegylated liposomal Doxorubicin: review of animal and human studies, *Clin. Pharmacokinet*, 2003, **42**, 419–436.

13 W. T. Al-Jamal, Z. S. Al-Ahmady and K. Kostarelos, Pharmacokinetics & tissue distribution of temperature-sensitive liposomal doxorubicin in tumor-bearing mice triggered with mild hyperthermia, *Biomaterials*, 2012, **33**, 4608–4617.

14 Z. S. Al-Ahmady, C. L. Scudamore and K. Kostarelos, Triggered doxorubicin release in solid tumors from thermosensitive liposome-peptide hybrids: Critical parameters and therapeutic efficacy, *Int. J. Cancer*, 2015, **137**, 731–743.
15 Z. S. Al-Ahmady, O. Chaloin and K. Kostarelos, Monoclonal antibody-targeted, temperature-sensitive liposomes: in vivo tumor chemotherapeutics in combination with mild hyperthermia, *J. Controlled Release*, 2014, **196**, 332–343.
16 D. Pozzi, G. Caracciolo, L. Digiacomo, V. Colapicchioni, S. Palchetti, A. L. Capriotti, C. Cavaliere, R. Zenezini Chiozzi, A. Puglisi and A. Lagana, The biomolecular corona of nanoparticles in circulating biological media, *Nanoscale*, 2015, **7**, 13958–13966.
17 D. Pozzi, V. Colapicchioni, G. Caracciolo, S. Piovesana, A. L. Capriotti, S. Palchetti, S. De Grossi, A. Riccioli, H. Amenitsch and A. Lagana, Effect of polyethyleneglycol (PEG) chain length on the bio-nano-interactions between PEGylated lipid nanoparticles and biological fluids: from nanostructure to uptake in cancer cells, *Nanoscale*, 2014, **6**, 2782–2792.
18 M. A. Dobrovolskaia, B. W. Neun, S. Man, X. Ye, M. Hansen, A. K. Patri, R. M. Crist and S. E. McNeil, Protein corona composition does not accurately predict hematocompatibility of colloidal gold nanoparticles, *Nanomedicine*, 2014, **10**, 1453–1463.
19 R. Gref, M. Luck, P. Quellec, M. Marchand, E. Dellacherie, S. Harnisch, T. Blunk and R. H. Muller, 'Stealth' corona-core nanoparticles surface modified by polyethylene glycol (PEG): influences of the corona (PEG chain length and surface density) and of the core composition on phagocytic uptake and plasma protein adsorption, *Colloids Surf., B*, 2000, **18**, 301–313.
20 S. M. Moghimi, I. S. Muir, L. Illum, S. S. Davis and V. Kolb-Bachofen, Coating particles with a block co-polymer (poloxamine-908) suppresses opsonization but permits the activity of dysopsonins in the serum, *Biochim. Biophys. Acta*, 1993, **1179**, 157–165.
21 S. Mishra, P. Webster and M. E. Davis, PEGylation significantly affects cellular uptake and intracellular trafficking of non-viral gene delivery particles, *Eur. J. Cell Biol.*, 2004, **83**, 97–111.
22 T. Fujita, Evolution of the lectin-complement pathway and its role in innate immunity, *Nat. Rev. Immunol.*, 2002, **2**, 346–353.
23 J. Szebeni, Complement activation-related pseudoallergy: a new class of drug-induced acute immune toxicity, *Toxicology*, 2005, **216**, 106–121.
24 A. Chanan-Khan, J. Szebeni, S. Savay, L. Liebes, N. M. Rafique, C. R. Alving and F. M. Muggia, Complement activation following first exposure to pegylated liposomal doxorubicin (Doxil): possible role in hypersensitivity reactions, *Ann. Oncol.*, 2003, **14**, 1430–1437.
25 J. Szebeni, F. Muggia, A. Gabizon and Y. Barenholz, Activation of complement by therapeutic liposomes and other lipid excipient-based therapeutic products: prediction and prevention, *Adv. Drug Delivery Rev.*, 2011, **63**, 1020–1030.
26 G. Caracciolo, D. Pozzi, A. L. Capriotti, C. Cavaliere, S. Piovesana, G. La Barbera, A. Amici and A. Lagana, The liposome-protein corona in mice and humans and its implications for in vivo delivery, *J. Mater. Chem. B*, 2014, **2**, 7419–7428.
27 S. Behzadi, V. Serpooshan, R. Sakhtianchi, B. Muller, K. Landfester, D. Crespy and M. Mahmoudi, Protein corona change the drug release profile of nanocarriers: the "overlooked" factor at the nanobio interface, *Colloids Surf., B*, 2014, **123**, 143–149.
28 G. Caracciolo, L. Callipo, S. C. De Sanctis, C. Cavaliere, D. Pozzi and A. Lagana, Surface adsorption of protein corona controls the cell internalization mechanism of DC-Chol-DOPE/DNA lipoplexes in serum, *Biochim. Biophys. Acta*, 2010, **1798**, 536–543.
29 M. Hadjidemetriou, N. Pippa, S. Pispas and C. Dernetzos, Incorporation of dimethoxycurcumin into charged liposomes and the formation kinetics of fractal aggregates of uncharged vectors, *J. Liposome Res.*, 2013, **23**, 94–100.
30 G. Caracciolo, F. Cardarelli, D. Pozzi, F. Salomone, G. Maccari, G. Bardi, A. L. Capriotti, C. Cavaliere, M. Papi and A. Lagana, Selective targeting capability acquired with a protein corona adsorbed on the surface of 1,2-dioleoyl-3-trimethylammonium propane/DNA nanoparticles, *ACS Applied Materials Interfaces*, 2013, **5**, 13171–13179.
31 A. Salvati, A. S. Pitek, M. P. Monopoli, K. Prapainop, F. B. Bombelli, D. R. Hristov, P. M. Kelly, C. Aberg, E. Mahon and K. A. Dawson, Transferrin-functionalized nanoparticles lose their targeting capabilities when a biomolecule corona adsorbs on the surface, *Nat. Nanotechnol.*, 2013, **8**, 137–143.
32 Z. S. Al-Ahmady, W. T. Al-Jamal, J. V. Bossche, T. T. Bui, A. F. Drake, A. J. Mason and K. Kostarelos, Lipid-peptide vesicle nanoscale hybrids for triggered drug release by mild hyperthermia in vitro and in vivo, *ACS Nano*, 2012, **6**, 9335–9346.
33 D. Needham, G. Anyarambhatla, G. Kong and M. W. Dewhirst, A new temperature-sensitive liposome for use with mild hyperthermia: characterization and testing in a human tumor xenograft model, *Cancer Res.*, 2000, **60**, 1197–1201.
34 G. Kong, G. Anyarambhatla, W. P. Petros, R. D. Braun, O. M. Colvin, D. Needham and M. W. Dewhirst, Efficacy of liposomes and hyperthermia in a human tumor xenograft model: importance of triggered drug release, *Cancer Res.*, 2000, **60**, 6950–6957.